

SHEAR THROUGH THE THICKNESS PROPERTY OF SCREW LAMINATED CROSS LAMINATED TIMBER

Shiro Nakajima¹

ABSTRACT: This paper focus on the shear through the thickness properties of screw laminated cross laminated timber. The shear through the thickness properties of screw laminated cross laminated timber was verified from the results of the shear through the thickness test. Four test specimens with different joint configuration and one test specimen with opening were tested to verify the effect of the number of joints and the length from the screwed joints to the center point of an over wrapping part of the laminations i.e. the length of the moment arm. The test results indicated that the shear through the thickness properties of screw laminated cross laminated timber depends on the number of screwed joints and the length of the moment arm. To estimate the shear through the thickness properties of screw laminated cross laminated timber a structural model and a calculation method were proposed. The load deformation curve of the screw laminated cross laminated timber derived from the proposed structural model and calculation method well estimated the test results at relatively small deformation level. The force caused by the embedment between the laminations brought a difference at the relatively large deformation level.

KEYWORDS: Shear through the thickness, Screw joint, Cross laminated timber, Structural modelling

1 INTRODUCTION

Cross laminated timber (CLT) is composed of sawn boards cross laminated and jointed with glue. The gluing procedure in manufacturing CLT requires high quality control to confirm adequate performance of gluing. And gluing also requires heavy-duty manufacturing facilities. Alternative methodologies for jointing sawn boards such as using mechanical joints will provide the possibility to simplify the manufacturing procedure of CLT and give a chance for relatively small mills to produce CLT.

The bending behaviour of nailed jointed CLT is reported by Sung-Jun Pang et.al [1]. And in Europe the Massiv-Holz-Mauer (MHM) is manufactured and the characteristic values of the panels are evaluated by European Technical Assessment [2]. To provide design methodologies and characteristic values for CLT composed of mechanically jointed laminations it is important to accumulate data and knowledge. This paper focus on the shear through the thickness properties of

screw laminated cross laminated timber (SL-CLT). Screw laminated cross laminated timber discussed in this paper is illustrated in Figure 1. The screw laminated cross laminated timber discussed in this paper is composed of lumbers of domestic species and the laminations are jointed with structural screws. The shear through the thickness properties of SL-CLT was verified from the results of the shear test. And the structural model and calculation method to evaluate the shear through the thickness properties of SL-CLT was proposed.

2 SHEAR THROUGH THE THICKNESS TEST

2.1 TEST SPECIMENS

The test specimens are composed of 3 layers of laminations. Each layer is composed of 15 laminations (sawn boards) sized 1800mm in length, 120mm in width and 30mm in thickness (see Figure 2). The species of the lumbers is Japanese Cedar (*Cryptomeria japonica*) of averaged MOE 9.76 (GPa). The detail characteristic

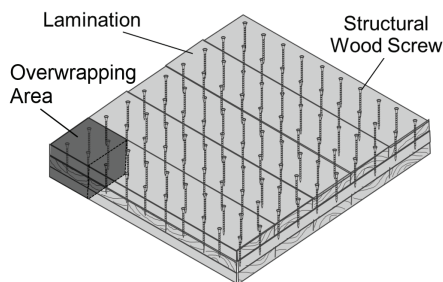


Figure 1: Screw laminated cross laminated timber (SL-CLT)

Table 1: Characteristic values of the lumber

	Average	Standard deviation
Density (kg/m ³)	386	35.8
MOE (kN/mm ²)	9.75	1.62
Moisture Contents (%)	10.0	1.30

¹ Shiro Nakajima, University of Utsunomiya, Japan, s-nakajima@cc.utsunomiya-u.ac.jp

values of the of the sawn boards composing the test specimens are given in Table.1.

Laminations of adjoining layers are jointed with structural wood screws 5mm in diameter and 80mm in length. The overwrapping parts of the adjoining laminations were jointed with 4 wood screws. The location of the joints is illustrated in Figure 2. There are two different joint configurations, Type A and Type B. Joint Type A has an edge distance of 20mm and for this edge distance the length of the moment arm is approximately 56.6mm. In this paper the moment arm is defined as the distance from the center of the overwrapping part of the adjoining laminations to the wood screw joints. For Type B the edge distance is 30mm and the length of the moment arm is approximately 43.4mm.

For test specimens Type 1 all the part the adjoining laminations overwrap are jointed with four structural wood screws. For test specimens Type 2 half of the overwrapping part are jointed with four structural wood screws. The number of wood screws used to compose the test specimen is 900 for test specimen Type 1 and 452 for test specimen Type 2. Test specimen Type 3 has an opening at the center of the panel and every overwrapping part are jointed with four structural wood screws. Five types of test specimens with different combination of length of the moment arm, number of screw joints and

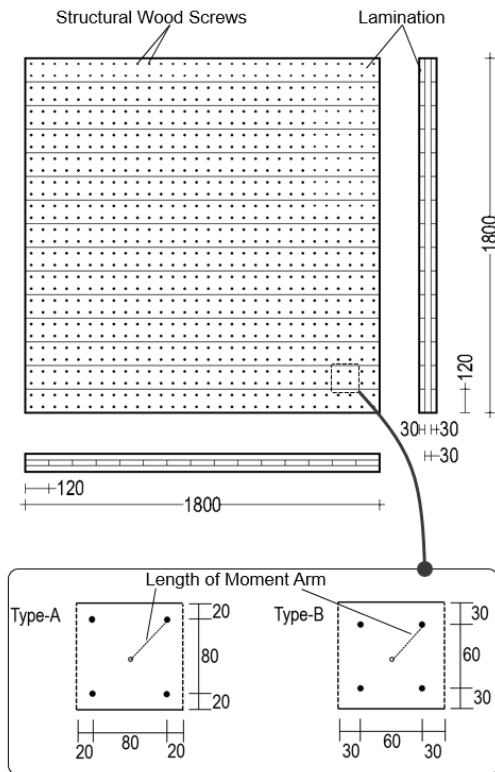


Figure 2: Configuration of the test specimens

Note: The figures in the square line shows the configuration of the joints at the overwrapping part of the laminations.

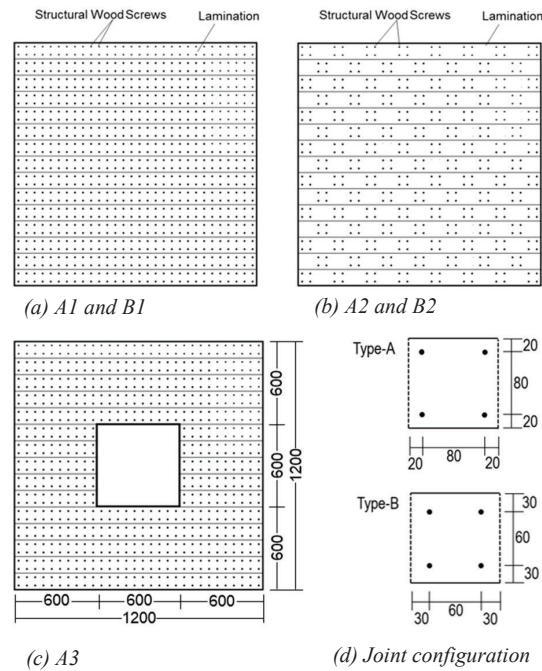


Figure 3: Type and symbol of the test specimens

existence of the openings were prepared and tested. The configuration of the five test specimens is given in Figure 3. All the overwrapping part of the laminations are jointed for test specimen A1 and B1 and the difference between the two test specimens is the length of the moment arm 56.6mm for A1 and 43.4mm for B1. And almost half of the overwrapping part of the laminations are jointed for test specimen A2 and B2 and the length of the moment arm is 56.6mm for A2 and 43.4mm for B2. Test specimen A3 has an opening at the center of the panel and the length of the moment arm is 56.6mm. All the overwrapping part of the laminations are jointed for test specimen A3.

2.2 TESTING METHOD

The setup of the shear through the thickness test is given in Figure 4. The out most layer of the laminations located at the top and bottom of the test specimens are extruded to a certain length to setup the test specimens to the testing facilities. And a girder was put on the top of the test specimens to adequately load to the test specimens. The left and right end of the girder were connected to the base frame of the testing equipment by tiedown rods. Reverse cyclic load was applied to the top of the test specimens. Three repetitive reverse cyclic load was applied at the shear deformation level of approximately 1.67×10^{-3} (1/600) rad, 2.22×10^{-3} (1/450) rad, 3.33×10^{-3} (1/300) rad, 6.67×10^{-3} (1/150) rad, 10.0×10^{-3} (1/100) rad, 13.3×10^{-3} (1/75) rad, 20.0×10^{-3} (1/50) rad, 33.3×10^{-3} (1/30) rad. And after this cyclic loading the test specimens were loaded to the shear deformation level 83.3×10^{-3} (1/15) rad.

The horizontal displacement of the top and bottom of the test specimens were measured and the vertical

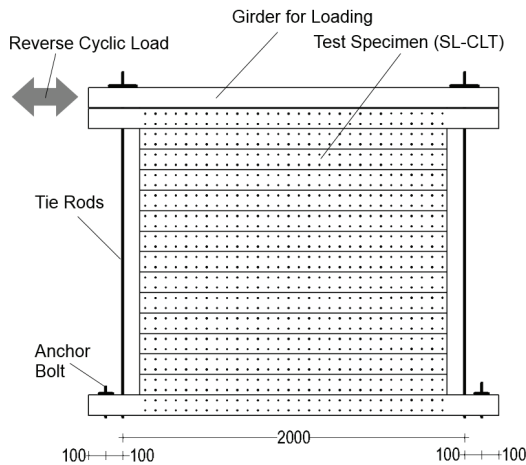


Figure 4: Setup of the shear through the thickness test

displacement at both left and right bottom of the test specimens were also measured. The rotation angle of the adjoining laminations was also measured at the vertical cut side of the test specimens.

3 TEST RESULTS

3.1 LOAD DEFORMATION CURVE

The envelope curves of the load deformation curves are given and compared in Figure 5. With an exception for

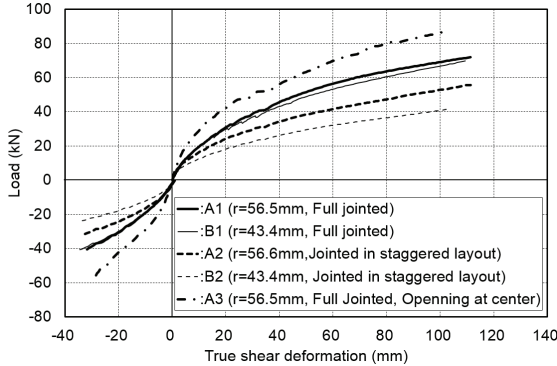


Figure 5: Envelope curves of the load deformation curves

Note: True shear deformation (δ_{true}) is calculated by the following formula.

$$\delta_{true} = \left(\frac{\delta_{h-top} - \delta_{h-bottom}}{H} - \frac{\delta_{v-act} - \delta_{v-free}}{L} \right) \times H$$

Where, δ_{h-top} is horizontal displacement at the top of the test specimen,
 $\delta_{h-bottom}$ is horizontal displacement at the bottom of the test specimen,
 δ_{v-act} is vertical displacement of the bottom edge the loaded side of test specimen,
 δ_{v-free} is vertical displacement of the bottom edge the unloaded side of test specimen,
 H is the height of the test specimen,
 L is the length of the test specimen.

test specimen A1 in general test specimens with longer moment arm length had higher load carrying capacity. And in general, the load carrying capacity was proportional to the number of joints.

3.2 LOAD DEFORMATION CURVE

The yield load (P_y), maximum load (P_{max}), ultimate load (P_u) and initial stiffness (K) are given in Table 2. Each characteristic value is assumed to has a positive correlation with the value obtained by multiplying the length of moment arm multiplied and the number of joints.

Table 2: Characteristic values of the SL-CLTs

Test specimens	Characteristic values			
	P_y (kN)	P_{max} (kN)	P_u (kN)	K (kN/mm)
A1	37.5	71.9	63.2	1.30
B1	35.8	69.8	60.0	1.25
A2	28.2	56.1	46.8	1.06
B2	21.1	41.5	35.1	0.81
A3	41.6	86.7	71.6	2.20

Note: Maximum load (P_{max}) is the load measured when the specimens had the true shear deformation of 6.67×10^{-3} rad..

The relationship between the values above mentioned and the characteristic values is given in Figure 6. With an exception for test specimen A1 the yield load, maximum load and ultimate load had a positive correlation with the value obtained by multiplying the moment arm length and the number of joints. And with an exception for test

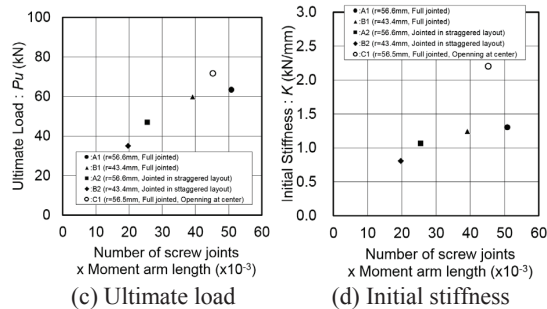
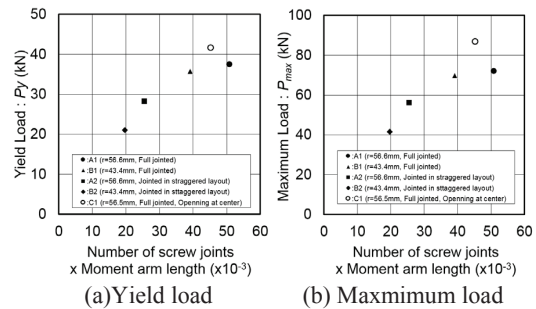
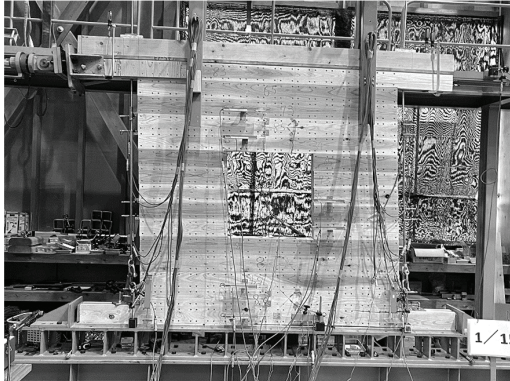


Figure 6: Relationship between each characteristic value and the value obtained by multiplying length of moment arm and number of joints

specimen A1 and B1 the initial stiffness had a positive correlation with the value obtained by multiplying the moment arm length and the number of joints.

3.3 DEFORMATION OF THE TEST SPECIMEN

Deformation of the test specimen A3 is shown as an example in Photo 1. The photo shows the deformation of the panel when the top of the panel was deformed to 120mm. Slippage can be observed between the vertically adjoining laminations.



(a) Deformation of the SL-CLT panel



(b) Slippage between the vertically adjoining laminations

Photo 1: Deformation of the SL-CLT panel A3

4 ESTIMATION OF LOAD DEFORMATION CURVE

4.1 MODELING AND CALCULATION

The deformation of the overlapping parts of the screw laminated CLT subjected to in-plane shear force can be model as shown in Figure 7.

When the SL-CLT panel has a shear deformation angle θ (rad) the deformation of the top of the panel x (mm) can be calculated by equation 1.

$$x = \theta \cdot (n \cdot H_{element}) \quad (1)$$

Where n is the number of lamination in vertical direction and $H_{element}$ is width of the lamination.

When the shear deformation angle of the panel is θ (rad) the shear force $F(\theta)$ (kN) generated at the screw joints can be calculated as equation 2.

$$F(\theta) = K_s(\theta) \cdot r \cdot \theta \quad (2)$$

Where $K_s(\theta)$ is shear stiffness of the screw joints at the shear deformation angle θ (rad) and r (mm) is the length of the moment arm.

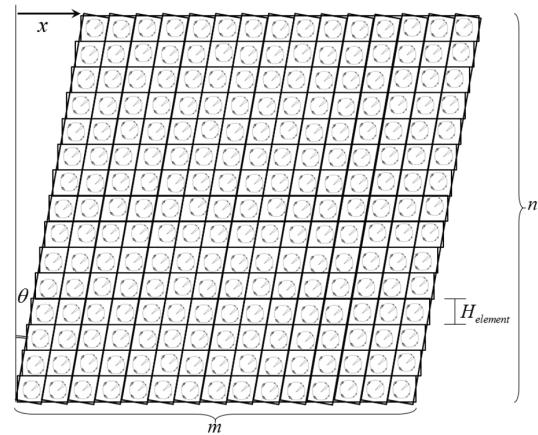
The internal energy consumption ($E_{INT}(\theta)$) caused by the shear deformation at a single screw joint can be calculated as equation 3.

$$E_{INT}(\theta) = \int_{\theta_1}^{\theta_2} F(\theta) \cdot \theta d\theta = \int_{\theta_1}^{\theta_2} K_s(\theta) \cdot r \theta d\theta \quad (3)$$

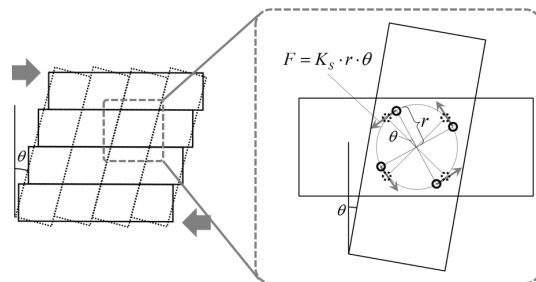
The number of screw joints N_s can be calculated by equation 4.

$$N_s = m \cdot n \cdot 4 \quad (4)$$

Where m is the number of lamination in horizontal direction, n is the number of lamination in vertical direction and 4 is the number of screw joints existing at one overlapping part. By inserting equation 4 to equation



(a) Structural model for SL-CLT



(b) Detail of the model

Figure 7: Structural modelling of SL-CLT

3 the internal energy consumption for the entire panel $E_{INT-total}(\theta)$ that is the energy consumed at all screw joints can be calculated as equation 5.

$$E_{INT-total}(\theta) = m \cdot n \cdot 4 \cdot \int_{\theta_1}^{\theta_2} K_S(\theta) \cdot r \theta d\theta \quad (5)$$

The external energy consumption $E_{EXT}(\theta)$ caused by the shear deformation θ (rad) of SL-CLT panel can be calculated as equation 6.

$$E_{EXT}(\theta) = \int_{x_1}^{x_2} P(x) \cdot x dx \quad (6)$$

$$= \int_{\theta_1}^{\theta_2} P \{ \theta \cdot (n \cdot H_{element}) \} \{ \theta \cdot (n \cdot H_{element}) \} d\theta$$

Where P is the load applied at the top of the SL-CLT panel. As $E_{INT-total}(\theta)$ is equal to $E_{EXT}(\theta)$ and the stiffness of the screw joint at a certain deformation level θ is known the load necessary to apply at the top of panel to give a certain deformation at the top of the panel can be calculated. By conducting an incremental displacement analysis, the load deformation curve of the SL-CLT panels was estimated.

4.2 LOAD DEFORMATION CURVE OF THE SCREW JOINT

The load deformation curve of the screw joint was derived from the test results of the joints. When a torsional deformation occurs at the overlapping part of the adjoining laminations the screw joints will deform at an

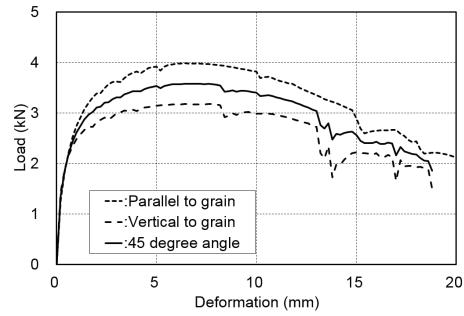


Figure 8: Load deformation curve the screw joints

angle of 45 degrees against the grain direction of wood. The load deformation curve for screw joint loaded at an angle of 45 degrees was estimated by the test results of screw joints loaded at parallel to grain and perpendicular to grain.

Figure 8 gives the load deformation curve of the screw joints. The load deformation curve for screw joint loaded at an angle of 45 degrees was calculated by the Hankinson's formula.

4.3 RESULTS OF CALCULATION

The results of the calculation are given in Figure 9 in comparison with the test results. With an exception for test specimen A1 the calculated load deformation curve well estimated the test results at deformation level

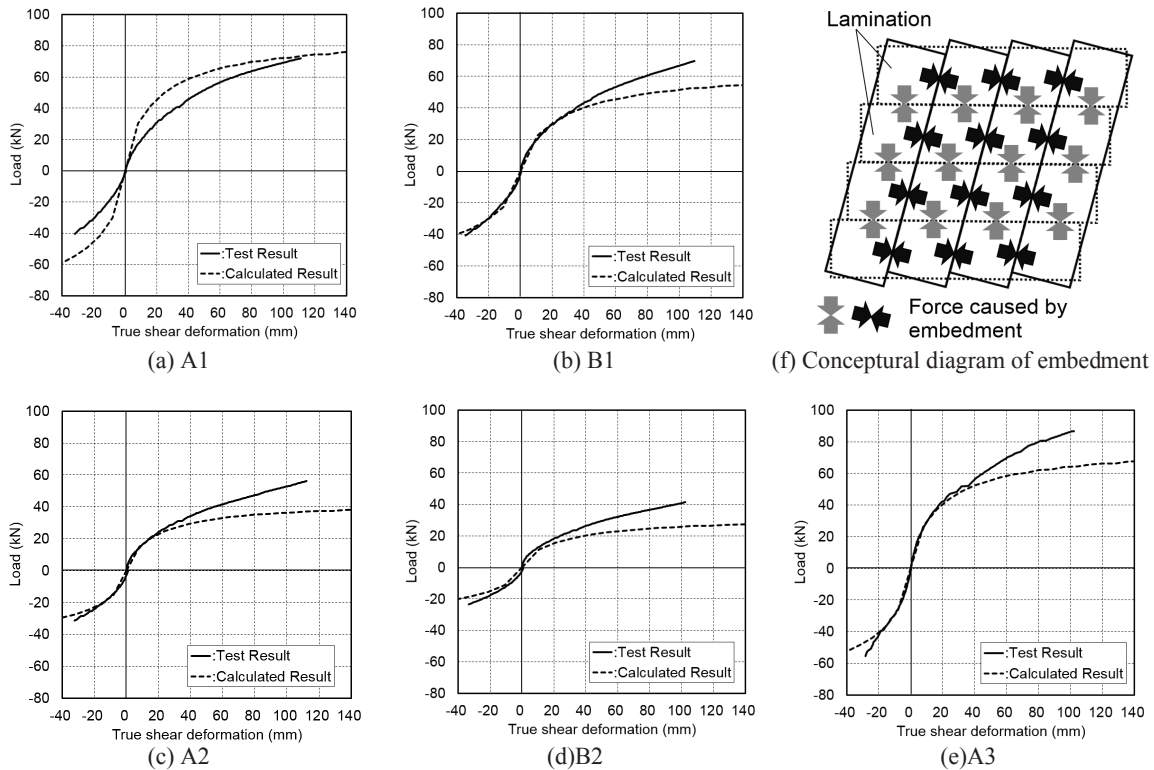


Figure 9: Load deformation curve, comparison of experimental results and calculated results

approximately up to 20mm. Though the load was under estimated when the deformation was approximately 20mm or more. The difference between the calculated load and measured load increased as the deformation increased. The reason for this difference is assumed as follows. When the shear deformation of the SL-CLT increase the gap between the laminations next to each other decrease. And as a result embedment will occur on the side face of the laminations. And the force derived by this embedment will increase as the shear deformation increase. Due to this embedment the load deformation curve calculated only by considering the force derived from the screw joints under estimate the load. The conceptual diagram of the embedment of laminations is given in Figure 9.

The difference between the measured and calculated load deformation curve of test specimen A1 was caused by the high moisture content of the lumbers composing the laminations. The test specimen A1 was manufactured with wet lumbers due to bad storage condition. And the lumbers dried and shrunk after being connected with structural wood screws. Small cracks may propagate and decreased the load carrying capacity of the joints but to conclude the correct reason further test should be conducted.

5 CONCLUSION

The shear through the thickness properties of screw laminated CLT was clarified through testing and the effect of the joint configuration on the shear stiffness was evaluated. A structural model and calculation method was proposed to estimate the load deformation curve. The proposed structural model and calculation method well estimated the load deformation relationship at a relatively small deformation level though at larger deformation level the load was under estimated. The force derived from the embedment between the laminations is supposed increased the load and led this under estimation. A model including the embedment characteristic of the laminations should be considered to accurately estimate the load deformation relationship of SL-CLT.

ACKNOWLEDGEMENT

This research was financially supported by the Maeda Engineering Foundation. The test was supported by Tochigi Prefecture Forest Research Center and Mr. Nobuya Namatame an undergraduate student of Utsunomiya University.

REFERENCES

- [1] Sung-Jun Pang, Kwang-Mo Kim, Sun-Hyang Park and Sang-Joon Lee. Bending behavior of nailed-jointed cross-laminated timber loaded perpendicular to plane. *Journal of Korean Wood Science*. 45(6):728-726, 2017.
- [2] European Technical Assessment, ETA-15/0760 of 27.04.2018, Austrian Institute of Construction Engineering.